Quantum-Behaved Particle Swarm Optimization-Tuned PI Controller of a SEPIC Converter

Sigit Dani Perkasa [1], Prisma Megantoro [2,*], Senit Araminta Jasmine [3]
[1,2] Faculty of Advanced Technology and Multidiscipline, Universitas Airlangga, Surabaya, Indonesia
[3] Electrical Engineering Department, National Sun Yat-Sen University, Kaohsiung, Taiwan
Email: [1] sigit.dani.perkasa-2020@ftmm.unair.ac.id, [2] prisma.megantoro@ftmm.unair.ac.id,
[3] m133610003@student.nsysu.edu.tw
*Corresponding Author

***Abstract*—The Single-Ended Primary Inductor Converter (SEPIC) is vital for voltage regulation in dynamic systems like renewable energy and electric vehicles. Traditional PI controllers struggle with tuning complexity and oscillations. This study introduces Quantum-Behaved Particle Swarm Optimization (QPSO) to optimize PI gains (Kp, Ki) for SEPIC converters. QPSO improves global search by using quantum-inspired probabilistic motion, overcoming issues of premature convergence seen in traditional PSO. Four objective functions—ISE, ITAE, IAE, and MSE—were evaluated to balance transient and steady-state performance. ITAE and IAE outperformed others, minimizing overshoot to 1.26% in boost mode and achieving the fastest settling time of 1,872 s. Sensitivity analysis revealed that Ki > 2.0 destabilizes the system, while Kp > 1.5 increases voltage ripples. The framework is computationally efficient, ideal for embedded applications. Future work should include hardware-in-loop testing to confirm robustness.**

***Keywords*—DC-DC Converter, PI Controller Tuning, Quantum-Behaved Particle Swarm Optimization, SEPIC, Steady State Accuracy, Transient Response**

I. INTRODUCTION

DC-DC converters, such as the Single-Ended Primary Inductor Converter (SEPIC), are critical for voltage regulation in renewable energy systems, electric vehicles, and battery management [1]. However, their performance is challenged by input voltage fluctuations, load variations, and nonlinear dynamics, necessitating advanced control strategies to ensure stability [2]. Specifically, SEPIC converters suffer from instability and reduced efficiency due to these fluctuating conditions, making advanced control strategies essential for maintaining stable operation. Traditional Proportional-Integral (PI) controllers, though widely used, often exhibit suboptimal transient response and steady-state accuracy due to manual tuning complexities and oscillation susceptibility during dynamic conditions [3]. Metaheuristic algorithms like Particle Swarm Optimization (PSO) have improved controller tuning but suffer from premature convergence to local optima in high-dimensional spaces [4]. Hybrid approaches (e.g., Grey Wolf Optimization-PSO) and emerging algorithms (e.g., Water Strider Optimization) address these limitations but lack global robustness in complex control landscapes [1], [5].

This study introduces Quantum-Behaved Particle Swarm Optimization (QPSO), a quantum mechanics-inspired variant of PSO, to optimize PI controller gains (Kp, Ki) for SEPIC converters. QPSO employs probabilistic particle motion guided by a mean best position (mbest), enhancing global exploration and mitigating stagnation [9]. While prior work demonstrates QPSO's efficacy in fractional-order PID control [10], its application to SEPIC systems—combined with a systematic evaluation of objective functions—remains unexplored. We rigorously compare four metrics: Integral of Squared Error (ISE), Integral of Time-Weighted Absolute Error (ITAE), Integral of Absolute Error (IAE), and Mean Squared Error (MSE), bridging a gap in understanding their trade-offs for SEPIC optimization [1], [6].

The key contributions are threefold: (1) a QPSO-based framework for global PI tuning in SEPIC converters, (2) identification of ITAE and IAE as optimal metrics for minimizing overshoot and settling time, and (3) validation of the framework's applicability to dynamic environments like renewable energy systems. The remainder of this paper details the SEPIC-QPSO methodology (Section II), presents results (Section III), discusses implications (Section IV), and concludes with future directions (Section V). This work bridges existing gaps by applying QPSO to SEPIC converter optimization, offering a fresh approach that is less prone to premature convergence. The introduction of ITAE and IAE metrics provides a clearer understanding of their trade-offs in optimizing SEPIC systems under varying operational conditions.

II. METHODOLOGY

A. System Configuration

1) SEPIC

The Single-Ended Primary Inductor Converter (SEPIC) is a DC-DC converter that regulates a fluctuating input voltage while maintaining a non-inverting output, making it ideal for applications with variable power sources [7]. The circuit of SEPIC is illustrated in Fig. 1.

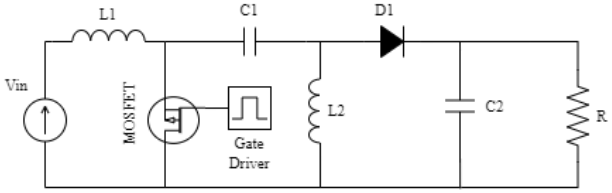

Fig. 1. SEPIC circuit

Based on the circuit in Fig. 1, the input inductor $L1$ stores energy when the MOSFET is ON and releases it when OFF, ensuring smooth current flow [8]. The coupling capacitor $C1$ transfers energy between the inductors while isolating the input from the output [9]. The output inductor $L2$ regulates

energy delivery to maintain a stable output [10]. The diode $D1$ provides a path for current when the MOSFET is OFF, preventing instability [11]. The output capacitor $C2$ filters voltage ripples, ensuring steady power [7]. The load resistor R represents the power-consuming element [8]. During MOSFET ON, $L1$ stores energy, $C1$ transfers energy to $L2$, and $D1$ is reverse-biased. When MOSFET OFF, $L1$ and $L2$ discharge, $D1$ conducts, and $C2$ stabilizes the output [9]. The component selection of the SEPIC used in this study follows:

$$I_{in_{max}} = \frac{P}{V_{in}} \tag{1}$$

$$I_{out_{max}} = \frac{P}{V_{out}} \tag{2}$$

$$R = \frac{V_{out}}{I_{out_{max}}} \tag{3}$$

$$\Delta I_{L1} = 0.01 \times I_{in_{max}} \tag{4}$$

$$\Delta I_{L2} = 0.01 \times I_{out_{max}} \tag{5}$$

$$\Delta V_{C1} = 0.01 \times V_{in} \tag{6}$$

$$\Delta V_{C2} = 0.01 \times V_{out} \tag{7}$$

$$L1 = \frac{V_{out} \cdot d}{\Delta I_{L1} \cdot f_s} \tag{8}$$

$$L2 = \frac{V_{out} \cdot d}{\Delta I_{L2} \cdot f_s} \tag{9}$$

$$C1 = \frac{d}{R \times \left(\frac{\Delta V_{C1}}{V_{out}}\right) \times f_s} \tag{10}$$

$$C2 = \frac{d}{R \times \left(\frac{\Delta V_{C2}}{V_{out}}\right) \times f_s} \tag{11}$$

Where $I_{in_{max}}$ and $I_{out_{max}}$ is the input and output current limits, $\Delta I_{L1}$and ΔI_{L2} is the current ripple for $L1$ and $L2$, ΔV_{C1} and ΔV_{C2} is the voltage ripple of the $C1$ and $C2$. Meanwhile d is the duty cycle and f_S is the switching frequency.

2) Closed Loop PI Controller

A closed-loop Proportional-Integral (PI) controller ensures stable operation of the SEPIC converter by dynamically adjusting the duty cycle to regulate the output voltage despite input or load variations [12]. The PI controller adjusts the duty cycle of the MOSFET to maintain the desired output voltage, compensating for any deviations caused by input voltage fluctuations or load variations. The closed-loop feedback system is shown in Fig. 2.

The system in Fig. 2 compares the reference voltage with the actual output to generate an error signal, which the PI controller processes [13]. The proportional term **(**Kp**)** provides an immediate response, while the integral term **(**Ki**)** eliminates steady-state errors over time, improving long-term stability [14]. The gains Kp and Ki are optimized using QPSO to minimize transient errors and steady-state deviations. These gains are adjusted dynamically based on real-time system feedback. These terms are summed to determine the necessary duty cycle adjustment [15]. The PWM generator converts the output of the PI controller into a duty cycle, controlling the MOSFET to adjust energy transfer, thereby stabilizing the output voltage. A higher duty cycle increases energy transfer, raising output voltage, while a lower duty cycle reduces it [16]. The SEPIC converter, controlled by this duty cycle, compensates for fluctuations to maintain a steady output [14].

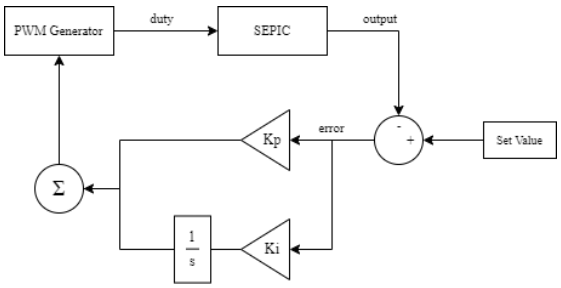

Fig. 2. Closed loop system with PI controller

B. Quantum-Behaved Particle Swarm Optimization

Quantum-Behaved Particle Swarm Optimization (QPSO) is an advanced variant of the classical Particle Swarm Optimization (PSO) algorithm. By incorporating principles from quantum mechanics, QPSO enhances search performance, global convergence, and exploration capabilities, making it more effective for complex optimization problems [17], [18]. Unlike classical PSO, which updates particle velocities based on fixed trajectories, QPSO introduces probabilistic particle motion guided by the mean best position (mbest), enhancing global search capabilities and reducing the risk of premature convergence in high-dimensional optimization problems. QPSO replaces the velocity update equation with a quantum wave function-based movement model, allowing probabilistic motion rather than a deterministic trajectory [17]. Instead of moving with velocity, each particle is attracted to a mean best position (*mbest*), defined as the average of all personal best positions:

$$x_i = pBest_i + \beta \cdot |mbest - x_i| \cdot ln(1/u) \tag{12}$$

Where x_i is the particle position, $pBest_i$ is the personal best position of each i, $mbest$ is the mean of all personal best positions, u is a random number in the range of 0 to 1, and β is a contraction-expansion coefficient that controls convergence speed [19]. By utilizing quantum principles, QPSO enables particles to explore a wider search space, avoiding local optima and improving global optimization efficiency [20], [21].

C. Objective Functions

To optimize the performance of the PI controller in the SEPIC converter, this research evaluates various performance metrics as objective functions. By comparing these metrics, the study aims to identify the optimal combination of K_p and K_i parameters using QPSO to produce the best transient response.

1) ISE

The Integral of Squared Error (ISE) is a widely used objective function for tuning PI controllers, minimizing system error over time while enhancing stability and transient response. ISE is defined as:

$$ISE = \int_0^T e^2(t)dt \quad (13)$$

Where $e(t)$ is the error signal, and T is the evaluation period. ISE penalizes larger errors more heavily, promoting fast settling time and reduced steady-state error [22]. It is commonly used in optimization-based control tuning, demonstrating effectiveness in improving system robustness and response characteristics [23], [24]. By minimizing ISE, the controller enhances voltage regulation accuracy and dynamic response in the SEPIC converter.

2) ITAE

The Integral of Time-Weighted Absolute Error (ITAE) is a widely used performance index for tuning PI controllers, prioritizing long-term accuracy and stability. ITAE assigns greater penalties to errors that persist over time, leading to improved transient response and overall system performance. It is mathematically defined as:

$$ITAE = \int_0^T t \cdot |e(t)|\, dt \quad (14)$$

Where t is the time variable. ITAE helps in reducing overshoot and settling time, making it a preferred criterion in control optimization [25]. It has been effectively applied in tuning controllers for various systems, ensuring enhanced stability and dynamic response [26].

3) IAE

The Integral of Absolute Error (IAE) is a widely used objective function for tuning PI controllers, aiming to minimize the total absolute error over time. By reducing error magnitude without emphasizing its duration, IAE improves overall system performance while maintaining a balance between transient response and steady-state accuracy. It is mathematically expressed as:

$$IAE = \int_0^T |e(t)|\, dt \quad (15)$$

IAE is frequently applied in control optimization, demonstrating effectiveness in enhancing system robustness and stability [22]. Studies have shown that selecting an appropriate objective function, such as IAE, significantly influences controller performance in various applications [6].

4) MSE

The Mean Squared Error (MSE) is a commonly used objective function for tuning PI controllers, aiming to minimize the average squared error between the desired and actual system outputs. By penalizing larger errors more heavily, MSE enhances system stability and overall control performance. It is mathematically defined as:

$$MSE = \frac{1}{T}\sum_{i=1}^{T} e(t)^2 \quad (16)$$

MSE is widely applied in optimization-based controller tuning, demonstrating effectiveness in improving tracking accuracy and dynamic response [27]. It has been successfully employed in various control applications, ensuring optimized performance through automated gain selection [5].

Each of the objective functions—ISE, ITAE, IAE, and MSE—is designed to evaluate different aspects of controller performance. ISE emphasizes fast settling and low steady-state error, ITAE prioritizes long-term stability with reduced overshoot, IAE minimizes the total absolute error, and MSE focuses on minimizing squared deviations for overall stability.

III. RESULTS

A. Sensitivity Analysis

Fig. 3 shows the sensitivity analysis results of the PI controller parameters using different performance metrics. Namely, 1(a) is ISE, 1(b) is ITAE, 1(c) is IAE, and 1(d) is MSE. Fig. 1 shows that optimal performance occurs around $K_p \approx 0.9$ and $K_i \approx 0.1$, where all error metrics are minimized. The lowest IAE (~50,000) at this tuning indicates minimal steady-state deviation, but it rises sharply to 500,000 at K_p = 2.0, and K_i = 4.0, highlighting poor regulation. Similarly, ISE is minimized at 2×10^6 for the optimal tuning but increases significantly to 2.5×10^7 for high gains, suggesting excessive oscillations. MSE follows the same trend, with a minimum value of 6 at $K_p \approx 0.9$ and $K_i \approx 0.1$, but exceeding 1,000 for unstable gain settings. Among these metrics, ITAE emerges as the most practical for real-time applications, balancing fast response and minimal long-term deviation. The lowest ITAE (~255,026) occurs at $K_p \approx 0.89$, $K_i \approx 0.1$, confirming this as the optimal tuning. However, ITAE rises above 2.5×10^5 at K_p = 2.0, and K_i = 4.0, indicating delayed error correction. The results suggest that increasing K_i beyond 2.0 leads to excessive oscillations and slow settling, while increasing K_p beyond 1.5 causes instability, significantly increasing ISE and MSE. The sensitivity analysis confirms that $K_p \approx 0.9$ and $K_i \approx 0.1$ provide the optimal balance between stability and response time for SEPIC converters.

B. Algorithm Behavior

1) Particle Generation

Fig. 4(a) to Fig. 4(d) reveals distinct tuning characteristics for K_p and K_i under different error metrics. For ISE, K_p starts high at approximately 2.0 and stabilizes around 0.05 after 10 iterations, while K_i at 5.0 and fluctuates between 2.5×10^5 and 3.5×10^5 after 20 iterations. This configuration achieves the fastest convergence and provides a stable response, making it effective for reducing squared error. Similarly, IAE leads to a lower final K_p (stabilizing at 0.03) compared to ISE, resulting in a less aggressive controller. However, Ki remains highly oscillatory within 1.5×10^5 to 3.5×10^5, which may cause integral windup issues. Although IAE prioritizes absolute error minimization, it struggles to stabilize K_i, potentially affecting long-term performance. In contrast, ITAE produces the smallest K_p, stabilizing at 0.02 after 20 iterations, indicating weak proportional control action. However, K_i fluctuates significantly between 1.0×10^5 and 4.5×10^5, making it the least stable among all methods. This excessive oscillation in integral gain suggests poor practical applicability due to erratic control behavior. Finally, MSE results in the lowest K_p (around 0.01 after 30 iterations),

making the controller the least aggressive. While K_i fluctuates between 1.5×10^5 and 3.0×10^5, it remains unstable, leading to slow response and potential integral windup. Despite reducing squared error, the MSE approach fails to achieve stable tuning, highlighting its limitations in buck mode operation. QPSO's ability to dynamically adjust particle positions ensures robust global optimization, preventing premature convergence and improving performance.

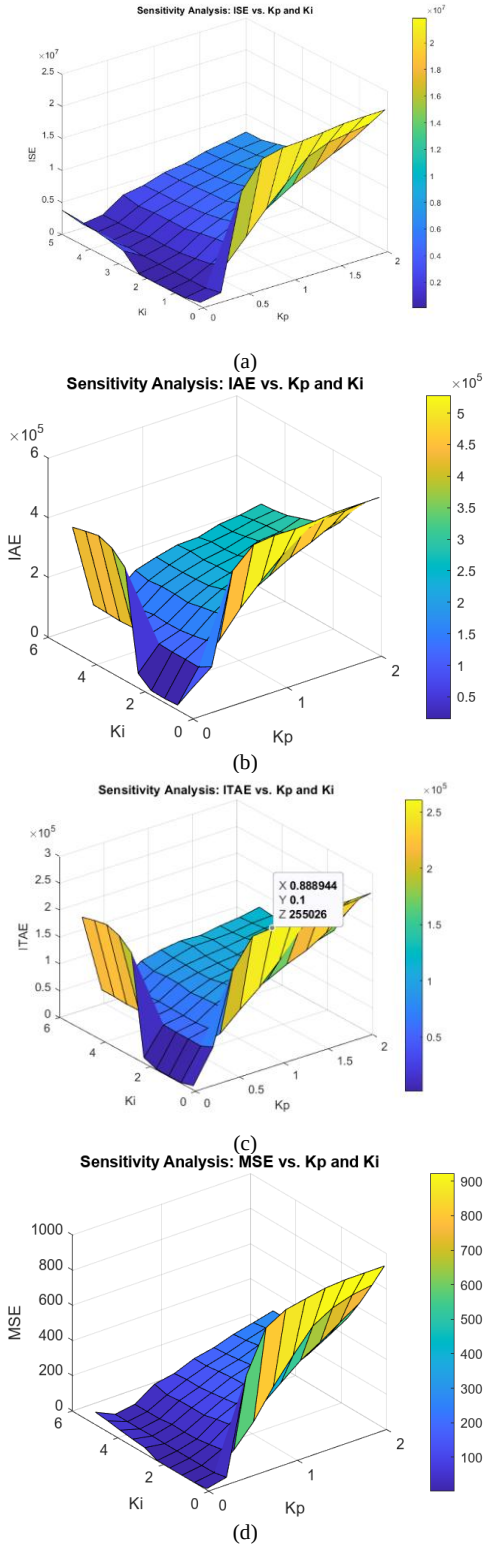

Fig. 3. PI controller parameters sensitivity analysis results against different performance metrics. (a) ISE (b) ITAE (c) IAE (d) MSE

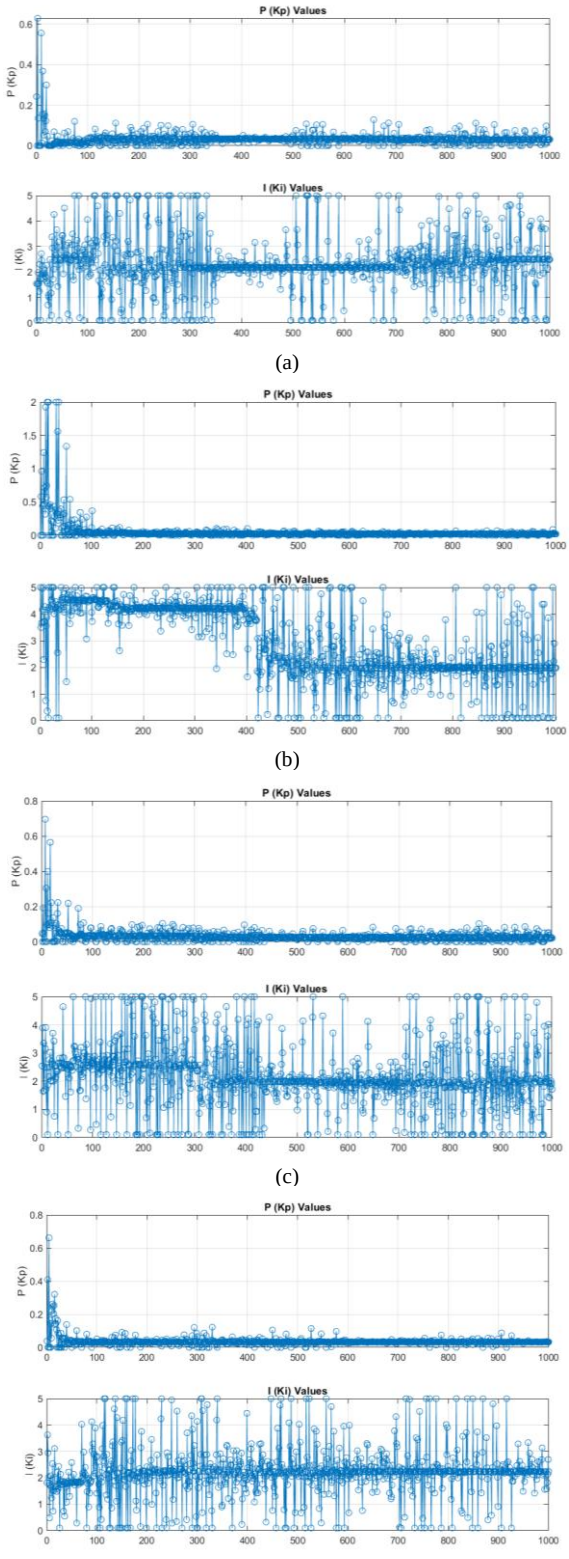

Fig. 4. Particle generation (K_p and K_i) using different performance metrics as objective functions (a) ISE (b) ITAE (c) IAE (d) MSE

2) Convergence

The convergence behavior of different error metrics in Fig. 5 reveals distinct optimization characteristics. ISE starts with an initial fitness of 2.1×10^6 and experiences a rapid decline in the first 10 iterations, reaching 1.3×10^6, before stabilizing at 1.2×10^6 after 30 iterations. This steep drop suggests fast optimization but indicates that ISE primarily

focuses on reducing squared error without strongly penalizing long-duration deviations. In contrast, ITAE exhibits the most aggressive reduction, dropping from an initial fitness of 11.5×10^4 to 6×10^4 within 10 iterations and further decreasing to 2×10^4 by iteration 40. This rapid decline highlights ITAE's effectiveness in minimizing time-weighted errors and achieving a low steady-state fitness. IAE demonstrates the slowest convergence, with its initial fitness of 2.2×10^5 remaining stagnant for the first 40 iterations, suggesting early-stage optimization difficulties. However, it improves significantly between iterations 60 and 80, converging at 1.6×10^5, indicating late-stage optimization success. MSE achieves the fastest convergence, dropping from 130 to 30 within 10 iterations and stabilizing at 20 after 30 iterations. While this suggests strong early-stage performance in minimizing squared deviations, it may not sufficiently emphasize long-term error behavior.

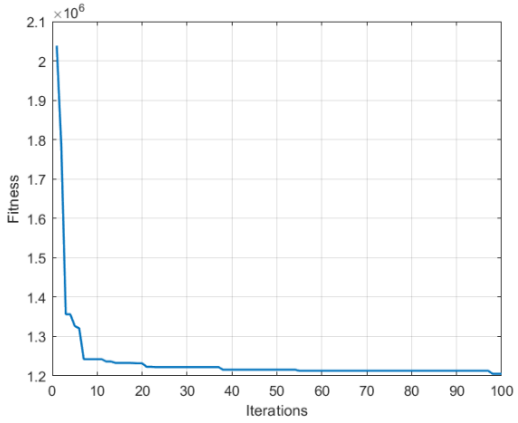

(a)

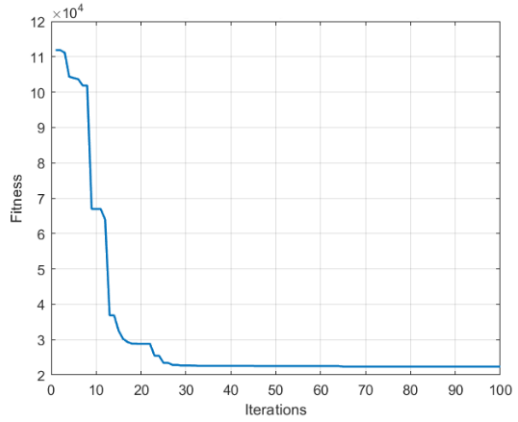

(b)

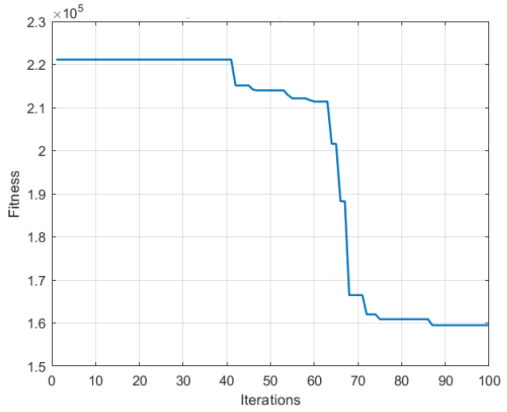

(c)

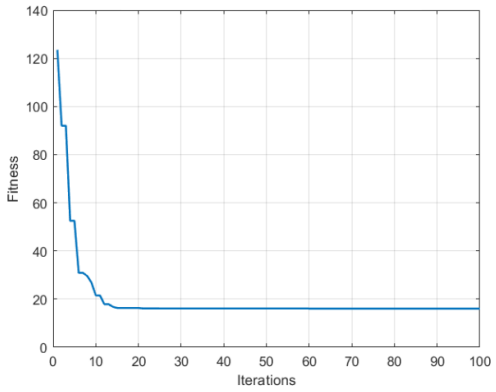

(d)

Fig. 5. Convergence curve of QPSO using different performance metrics as objective function. (a) ISE (b) ITAE (c) IAE (d) MSE

C. Transient Response

1) Buck Mode

Fig. 6 shows the transient response of the SEPIC converter in buck mode with QPSO PI controller with different performance metrics as objective function, the IAE-based controller demonstrates the best performance, achieving a faster settling time with moderate peak overshoot (28.99%) and a balanced steady-state error (SSE = 22936.21). The ITAE-based controller also performs well, exhibiting the lowest peak overshoot (18.99%) while maintaining a similar SSE (24526.66). Meanwhile, the ISE- and MSE-based controllers show excessive oscillations, with ISE peaking at 48.17% and MSE at 50.48%, making them less favorable choices for ensuring stability. The inset zoomed-in region confirms that IAE and ITAE provide smoother and more stable responses, making them the most suitable for buck operation.

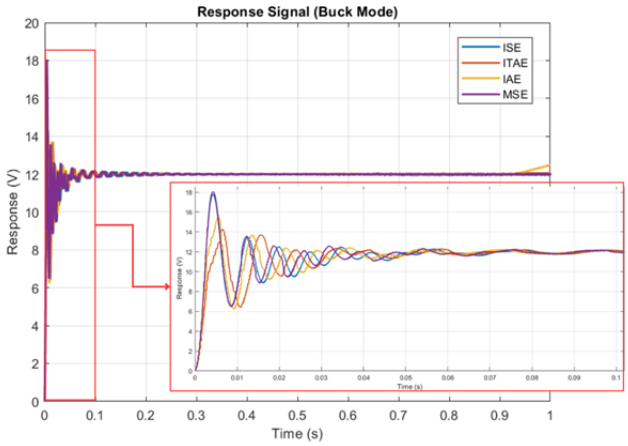

Fig. 6. QPSO-tuned PID controlled SEPIC converter response on buck mode

2) Boost Mode

Fig. 7 shows the transient response of the SEPIC converter in boost mode with QPSO PI controller with different performance metrics as objective function. IAE and ITAE deliver nearly identical performance, with IAE showing a peak overshoot of 1.62% and ITAE achieving the lowest at 1.26%. The MSE-based controller exhibits the worst performance, with a peak overshoot of 26.95%, indicating poor stability. The response curves show that IAE achieves the fastest settling, while ITAE ensures minimal

overshoot. Both are significantly better than the ISE-based controller, which has a higher overshoot and slower convergence. The inset highlights that ITAE achieves the smoothest rise, while IAE balances both speed and accuracy, making them the best choices for boost operation.

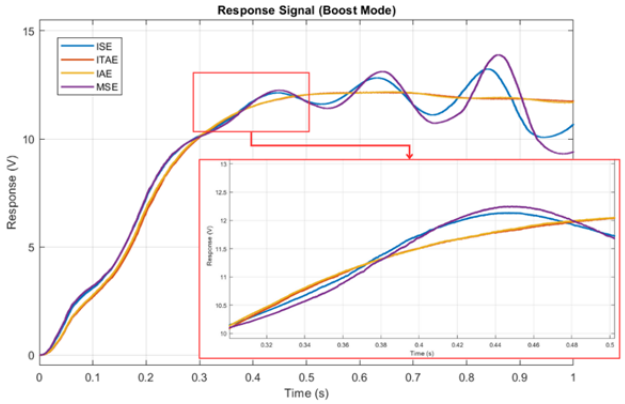

Fig. 7. QPSO-tuned PID controlled SEPIC converter response on buck mode

The comparison of transient response in Table 1 confirms the observations from the transient response figures, showing that IAE consistently results in the shortest simulation time in both buck (2376.33s) and boost (1872.19s) modes, making it the most computationally efficient. ITAE performs similarly but takes slightly longer (2491.30s in buck and 2420.47s in boost), while achieving the lowest peak overshoot in both cases. The MSE-based controller performs the worst overall, with the highest overshoot (50.48% in buck, 26.95% in boost) and longest simulation time (2406.04s in buck, 3449.92s in boost). The SSE values further highlight that IAE and ITAE are the best choices, as they minimize error while maintaining system stability. The transient response tests highlight that the IAE-based controller is the most effective in achieving rapid settling with minimal overshoot, making it ideal for high-performance applications.

Table 1. Transient response performance table

	Buck				Boost			
	ISE	**ITAE**	**IAE**	**MSE**	**ISE**	**ITAE**	**IAE**	**MSE**
T tot (s)	2853.56	2491.30	2376.33	2406.04	3008.92	2420.47	1872.19	3449.92
T avg (s)	28.53	24.91	23.76	24.06	30.08	24.20	18.72	34.49
K_p	0.032563	0.020362	0.025021	0.033026	0.017434	0.014692	0.014846	0.018206
K_i	2.0843	1.9805	1.9876	2.2348	0.34021	0.32308	0.32448	0.34581
Tr	0.0025	0.0031	0.0028	0.0025	0.3392	0.3302	0.33	0.3418
PO	48.171	18.9945	28.9866	50.4751	13.295	1.2574	1.6246	26.9516
SSE	22912.46	24526.66	22936.21	22578.09	1205304.04	1288623.72	1263690.64	1240233.02

IV. DISCUSSION

The integration of Quantum-Behaved Particle Swarm Optimization (QPSO) with a PI-controlled SEPIC converter demonstrates that objective function selection profoundly impacts transient and steady-state performance. ITAE and IAE outperformed ISE and MSE, balancing rapid response and stability. ITAE minimized overshoot (18.99% in buck, 1.26% in boost) by penalizing persistent errors (Fig. 3b, 7), while IAE achieved the fastest settling times (2,376.33 s in buck, 1,872.19 s in boost) through absolute error mitigation (Table 1). In contrast, ISE and MSE induced oscillations (e.g., 50.48% overshoot for MSE in buck mode) due to their quadratic emphasis on deviations, highlighting the need for application-specific metric alignment. These results align with prior studies advocating time-domain metrics for power electronics control.

QPSO's quantum-inspired mechanics, including mbest-guided exploration equation (12), enabled robust global optimization. The algorithm's rapid fitness reduction (e.g., ITAE dropping from 11.5×10^4 to 2×10^4 in 40 iterations, Fig. 5b) underscores its superiority over classical methods in nonlinear parameter spaces. However, oscillatory Ki values under ITAE/IAE (Fig. 4b–c) suggest adaptive tuning of QPSO's contraction-expansion coefficient (β) could enhance stability.

Practically, the proposed optimized SEPIC converter holds promise for renewable energy and electric vehicle systems, where ITAE's minimal overshoot mitigates voltage stress, and IAE's computational efficiency suits embedded platforms. However, the absence of hardware-in-loop validation or parasitic effect inclusion limits direct applicability. Future work must address these gaps while extending the framework to multi-objective scenarios (e.g., minimizing settling time and component stress) and benchmarking against hybrid quantum-classical algorithms. QPSO paired with ITAE/IAE provides a robust methodology for SEPIC control, balancing dynamic and steady-state performance. This approach advances adaptive power converter design, offering a scalable foundation for energy systems facing operational uncertainties.

V. CONCLUSION

This study establishes Quantum-Behaved Particle Swarm Optimization (QPSO) as an effective method for tuning PI controllers in SEPIC converters, with ITAE and IAE emerging as optimal objective functions for balancing transient response (e.g., 1.26% overshoot in boost mode) and steady-state accuracy. While ISE and MSE induced oscillations (up to 50.48% overshoot), ITAE and IAE minimized deviations and achieved rapid settling (1,872.19s in boost mode), demonstrating their superiority for power electronics applications. QPSO's quantum-inspired mechanics enabled robust global convergence, though adaptive tuning of its parameters could further stabilize integral gains. The framework holds promise for renewable energy and electric vehicle systems, though future work must validate results through hardware-in-loop testing and extend

optimization to multi-objective scenarios. This approach advances adaptive DC-DC converter design, offering a scalable solution for voltage regulation in dynamic environments.

ACKNOWLEDGMENT

The Authors would like to express our sincere gratitude to the Research Centre for New and Renewable Energy Engineering, Universitas Airlangga, for providing the resources and support necessary for the successful completion of this study.

REFERENCES

[1] A. B. Kancherla, N. B. Prasad, and D. R. Kishore, "Hybrid-optimized PI Controller With SEPIC Converter in PV-Based Grid-Integrated Electric Vehicle," *2023 International Conference on Signal Processing, Computation, Electronics, Power and Telecommunication (IConSCEPT)*, *IEEE*, pp. 1–5, 2023, https://doi.org/10.1109/IConSCEPT57958.2023.10170601.

[2] Md. R. K. Shagor, A. J. Mahmud, M. M. Nishat, F. Faisal, M. H. Mithun, and Md. A. Khan, "Firefly Algorithm Based Optimized PID Controller for Stability Analysis of DC-DC SEPIC Converter," in *2021 IEEE 12th Annual Ubiquitous Computing, Electronics & Mobile Communication Conference (UEMCON)*, *IEEE*, pp. 0957–0963, 2021, https://doi.org/10.1109/UEMCON53757.2021.9666555.

[3] F. M. Kirikci, Ö. Akyazi, and H. Kahveci, "WSO-Optimized PID Controller Design for SEPIC Converter Voltage Stability," *2024 8th International Artificial Intelligence and Data Processing Symposium (IDAP)*, *IEEE*, pp. 1–6, 2024, https://doi.org/10.1109/IDAP64064.2024.10710743.

[4] U. Shukla, S. Yadav, N. Tiwari, and A. Priyadarshini, "Optimisation of PI controller for design and modelling of Cuk, forward, and SEPIC converter," *International Journal of Power Electronics*, vol. 18, no. 2, pp. 201–234, 2023, https://doi.org/10.1504/IJPELEC.2023.132978.

[5] T. A. Naidu, S. R. Arya, R. Maurya, and P. Sanjeevikumar, "Variable fractional power-least mean square based control algorithm with optimized PI gains for the operation of dynamic voltage restorer," *IET Power Electronics*, vol. 14, no. 4, pp. 821–833, 2021, https://doi.org/10.1049/pel2.12067.

[6] W. Zhang, H. Dong, Y. Xu, D. Cao, and X. Li, "Multiobjective Tuning and Performance Assessment of PID Using Teaching–Learning-Based Optimization," *ACS Omega*, vol. 6, no. 47, pp. 31765–31774, 2021, https://doi.org/10.1021/acsomega.1c04428.

[7] E. Babaei and M. E. Seyed Mahmoodieh, "Calculation of Output Voltage Ripple and Design Considerations of SEPIC Converter," *IEEE Transactions on Industrial Electronics*, vol. 61, no. 3, pp. 1213–1222, 2014, https://doi.org/10.1109/TIE.2013.2262748.

[8] H. Suryoatmojo, I. Dilianto, Suwito, R. Mardiyanto, E. Setijadi, and D. C. Riawan, "Design and analysis of high gain modified SEPIC converter for photovoltaic applications," *2018 IEEE International Conference on Innovative Research and Development (ICIRD)*, *IEEE*, pp. 1–6, 2018, https://doi.org/10.1109/ICIRD.2018.8376319.

[9] A. Sel and C. Kasnakoglu, "Design of extended Kalman filter for SEPIC converter and comparison to Kalman filter," *SN Applied Sciences*, vol. 2, no. 4, p. 536, 2020, https://doi.org/10.1007/s42452-020-2347-6.

[10] P. K. Maroti, S. Padmanaban, J. B. Holm-Nielsen, M. Sagar Bhaskar, M. Meraj, and A. Iqbal, "A New Structure of High Voltage Gain SEPIC Converter for Renewable Energy Applications," *IEEE Access*, vol. 7, pp. 89857–89868, 2019, https://doi.org/10.1109/ACCESS.2019.2925564.

[11] S. M. Taheri, A. Baghramian, and S. A. Pourseyedi, "A Novel High-Step-Up SEPIC-Based Nonisolated Three-Port DC–DC Converter Proper for Renewable Energy Applications," *IEEE Transactions on Industrial Electronics*, vol. 70, no. 10, pp. 10114–10122, 2023, https://doi.org/10.1109/TIE.2022.3220909.

[12] A.-K. Daud and S. Khader, "Closed Loop Modified SEPIC Converter for Photovoltaic System," *Wseas Transactions on Circuits and Systems*, vol. 21, pp. 161–167, 2022, https://doi.org/10.37394/23201.2022.21.17.

[13] A. K. Singh, M. A. Chaudhari, R. Kumar, and K. S. R. Sekhar, "Closed Loop Control of Isolated SEPIC Converter for EV Charging," *2023 IEEE International Conference on Power Electronics, Smart Grid, and Renewable Energy (PESGRE)*, *IEEE*, pp. 1–6, 2023, https://doi.org/10.1109/PESGRE58662.2023.10404233.

[14] S. Mouslim, M. Oubella, M. Kourchi, and M. Ajaamoum, "Simulation and analyses of SEPIC converter using linear PID and fuzzy logic controller," *MaterialsToday: Proceedings*, vol. 27, pp. 3199–3208, 2020, https://doi.org/10.1016/j.matpr.2020.04.506.

[15] S. I. Khather and M. A. Ibrahim, "Modeling and simulation of SEPIC controlled converter using PID controller," *International Journal of Power Electronics and Drive Systems (IJPEDS)*, vol. 11, no. 2, p. 833, 2020, https://doi.org/10.11591/ijpeds.v11.i2.pp833-843.

[16] M. Duraisamy, "Closed-loop Implementation of a Non-isolated High Step-up Integrated SEPIC-CUK DC-DC Converter Structure with Single Switch," *Brazilian Archives of Biology and Technology*, vol. 67, 2024, https://doi.org/10.1590/1678-4324-2024230787.

[17] V. S. Rugveth and K. Khatter, "Sensitivity analysis on Gaussian quantum-behaved particle swarm optimization control parameters," *Soft Computing*, vol. 27, no. 13, pp. 8759–8774, 2023, https://doi.org/10.1007/s00500-023-08011-4.

[18] X. Li, W. Fang, and S. Zhu, "An improved binary quantum-behaved particle swarm optimization algorithm for knapsack problems," *Information Sciences*, vol. 648, p. 119529, 2023, https://doi.org/10.1016/j.ins.2023.119529.

[19] T. Yan and F. Liu, "Quantum-Behaved Particle Swarm Optimization Algorithm Based on the Two-Body Problem," *Chinese Journal of Electronics*, vol. 28, no. 3, pp. 569–576, 2019, https://doi.org/10.1049/cje.2019.03.023.

[20] M. Li, D. Cao, and H. Gao, "A Quantum Behaved Particle Swarm Optimization with a Chaotic Operator," *International Symposium on Artificial Intelligence and Robotic*, pp. 212–218, 2024, https://doi.org/10.1007/978-981-99-9109-9_21.

[21] A. S. Bhatia, M. K. Saggi, and S. Zheng, "QPSO-CD: quantum-behaved particle swarm optimization algorithm with Cauchy distribution," *Quantum Information Processing*, vol. 19, no. 10, p. 345, 2020, https://doi.org/10.1007/s11128-020-02842-y.

[22] S. A. N. Burnaz and M. Ş. Ayas, "Effects of objective function in PID controller design for an AVR system," *International Journal of Applied Mathematics Electronics and Computers*, vol. 8, no. 4, pp. 245–255, 2020, https://doi.org/10.18100/ijamec.803257.

[23] M. A. El-Dabah, S. Kamel, M. A. Y. Abido, and B. Khan, "Optimal tuning of fractional-order proportional, integral, derivative and tilt-integral-derivative based power system stabilizers using Runge Kutta optimizer," *Engineering Reports*, vol. 4, no. 6, 2022, https://doi.org/10.1002/eng2.12492.

[24] A. A. M. Zahir, S. S. N. Alhady, A. A. A. Wahab, and M. F. Ahmad, "Objective functions modification of GA optimized PID controller for brushed DC motor," *International Journal of Electrical and Computer Engineering (IJECE)*, vol. 10, no. 3, p. 2426, 2020, https://doi.org/10.11591/ijece.v10i3.pp2426-2433.

[25] A. F. Güven and O. Ö. Mengi, "Nature-ınspired algorithms for optimizing fractional order PID controllers in time-delayed systems," *Optimal Control Applications and Methods*, vol. 45, no. 3, pp. 1251–1279, 2024, https://doi.org/10.1002/oca.3101.

[26] M. Z. Mohd Tumari, M. A. Ahmad, M. H. Suid, and M. R. Hao, "An Improved Marine Predators Algorithm-Tuned Fractional-Order PID Controller for Automatic Voltage Regulator System," *Fractal and Fractional*, vol. 7, no. 7, p. 561, 2023, https://doi.org/10.3390/fractalfract7070561.

[27] M. S. Can and H. Ercan, "Real-time tuning of PID controller based on optimization algorithms for a quadrotor," *Aircraft Engineering and Aerospace Technology*, vol. 94, no. 3, pp. 418–430, 2022, https://doi.org/10.1108/AEAT-06-2021-0173.